

Regulation of membrane scission in yeast endocytosis

Deepikaa Menon¹ and Marko Kaksonen^{1*}

*For correspondence:

Marko.Kaksonen@unige.ch ()

¹Department of Biochemistry, University of Geneva, Geneva, Switzerland

Abstract

Introduction

In Clathrin-mediated endocytosis, a flat plasma membrane is pulled into a tubular invagination that eventually forms a vesicle. Forces that drive the transition from invagination to spherical vesicle in mammalian cells are provided by constriction of the GTPase Dynamin. Dynamin is now known to act in concert with the crescent-shaped N-BAR proteins Endophilin and Amphiphysin (ref. Dynamin papers). Proline-rich motifs on the Dynamin. In yeast cells, what causes membrane scission is unclear, although the yeast N-BAR protein complex Rvs has been identified as an important component of the scission module. In yeast, the Amphiphysin and Endophilin homologue Rvs is a heterodimeric complex composed of Rvs161 and Rvs167 (Friesen et al., 2006). Deletion of Rvs reduces scission efficiency by nearly 30% and reduces the invagination lengths at which scission occurs (ref Marko, wanda). Apart from a canonical N-BAR domain which forms a crescent-shaped structure, Rvs167 has a Glycine-Proline-Alanine rich (GPA) region and a C-terminal SH3 domain. Rvs161 and Rvs167 N-BAR domains are 42% similar, and 21% identical, but are not interchangeable (Sivadon, Crouzet and Aigle, 1997). The GPA region is thought to act as a linker with no known other function, while loss of the SH3 domain affects budding pattern and actin morphology. Most Rvs deletion phenotypes can however, be rescued by expression of the BAR domain alone (Sivadon, Crouzet and Aigle, 1997), suggesting that the BAR domains are the main functional unit of the Rvs complex. Homology modelling has shown that the BAR domain of Rvs167 is similar to Amphiphysin and Endophilin (Youn et al., 2010), and is therefore likely to function similarly to the mammalian homologues. In keeping with this theory, Rvs has been shown to tubulate liposomes in vitro (Youn et al., 2010). The Rvs complex arrives at endocytic sites in the last stage of the endocytosis, and disassembles rapidly at the time of membrane scission (Picco et al., 2015), consistent with a role in membrane scission. While it is known to be involved in the last stages of endocytosis, a mechanistic understanding of the influence of Rvs on scission however, remains incomplete. u89

We used quantitative live-cell imaging and genetic manipulation in *S.cerevisiae* to investigate the influence of Rvs and several Rvs interacting proteins that have been suggested to have a role in scission. We found that arrival of Rvs to endocytic sites is timed by interaction of its BAR domain with a specific membrane curvature. The Rvs167 SH3 domain affects localization efficiency of the Rvs complex and also influences invagination dynamics. This indicates that both BAR and SH3 domains are important for the role of Rvs as a regulator of scission. We tested current models of membrane scission, and find that deleting yeast synaptojanins or dynamin does not change scission dynamics. Interfacial forces at lipid boundaries are therefore unlikely to be sufficient for scission, and forces exerted by dynamin are not required. Furthermore, invagination length is insensitive to overexpression of Rvs, suggesting that the recently proposed mechanism of BAR-induced protein friction on the membrane is not likely to drive scission. We propose that recruitment of Rvs BAR

domains prevents scission and allows invaginations to grow by stabilizing them. We also propose that vesicle formation is dependent on forces exerted by a different module of the endocytic pathway, the actin network. Preventing premature membrane scission via BAR interaction could allow invaginations to grow to a particular length and accumulate enough forces within the actin network to reliably cut the membrane.

Results

Removal of Rvs167, not Vps1, results in reduced coat movement

Yeast Dynamin-like protein Vps1 does not contain the canonical Proline Rich Domain, which in mammalian cells is required for recruitment to endocytic sites (ref Grabs et al., 1997; Cestra et al., 1999; Farsad et al., 2001; Meinecke et al., 2013). Some work has reported its recruitment at endocytic proteins (ref Ayscough, Yu, 2004; Nannapaneni et al., 2010). Vps1 tagged both N- and C-terminally with GFP constructs failed to co-localize with endocytic protein Abp1 in our hands (Fig.1 supplement), consistent with other work that observed localization only with other parts of the trafficking pathway (ref Gadila 2017).

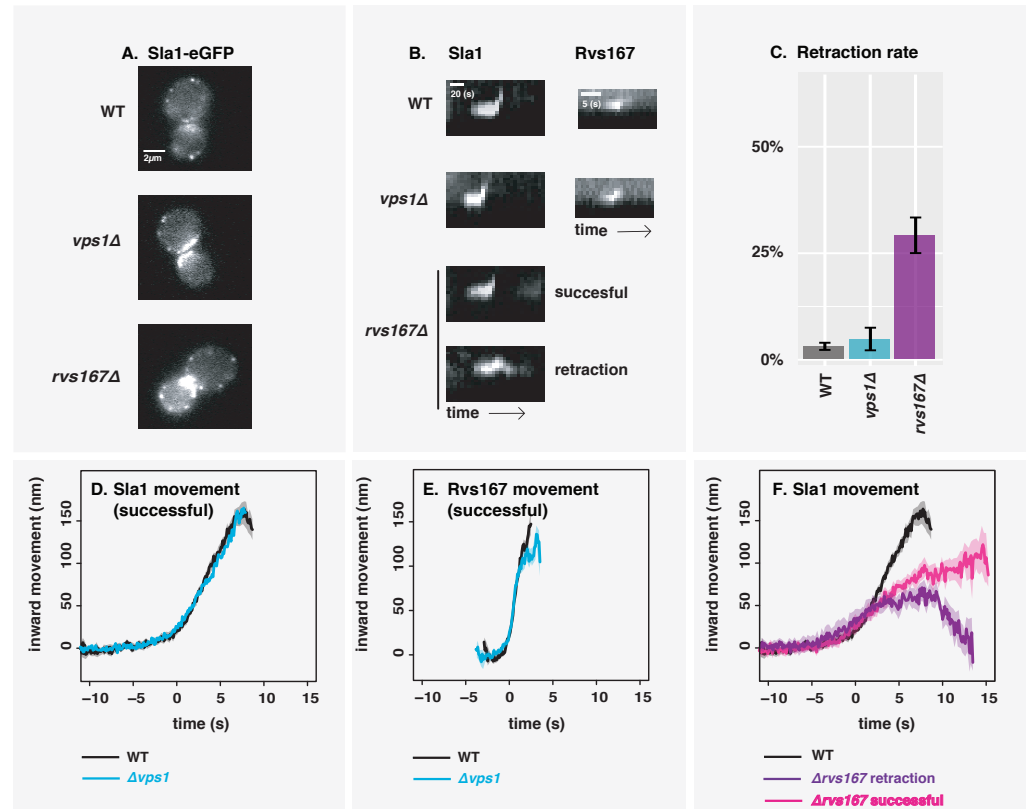


Figure 1. A: Slice from image of WT, *vps1Δ*, and *rvs167Δ* cells expressing Sla1-eGFP. Scale bar= 2μm. B: Representative kymographs of Sla1-eGFP and Rvs167-eGFP patches in WT, *vps1Δ*, and *rvs167Δ* cells. Scale bar for Sla1-egfp = 20(s), scale bar for Rvs167-eGFP = 5(s). C: Histogram of Sla1-eGFP retraction percentages in WT, *vps1Δ*, and *rvs167Δ* cells. Error bars are standard deviation from two data sets, $p < 0.001 = *$. D: Averaged centroid positions of Sla1-eGFP in WT and *vps1Δ* cells. E: Averaged position of Rvs167-eGFP in WT and *vps1Δ* cells. F: Averaged position of Sla1-eGFP in WT, and successful and retracted Sla1-eGFP positions in *rvs167Δ* cells. All averaged positions are aligned in time to begin inward movement at the same time=0(s), and aligned in space to a starting position = 0(nm). Note that in E, averaged Rvs167-eGFP inward movement is concomitant with the maxima of its fluorescent intensity (Fig1.supplement3)

To test whether absence of Vps1 influences scission, dynamics of endocytosis are observed in

58 cells lacking Vps1 and compared against wild-type (WT) cells (Fig.1A-F). Vps1 deletion is confirmed
59 by sequencing the open reading frame, and these cells show a growth phenotype at 37°C (Fig.1,
60 supplement2) that has been previously reported (ref. ayscough). Rates of retraction of the mem-
61 brane in *vps1Δ* and WT cells is quantified by tracking the endocytic coat protein Sla1 tagged at
62 the C-terminus with eGFP (Fig.1C). Upon actin polymerization, the endocytic coat is pulled into
63 the cytoplasm along with the membrane as it invaginates (ref.Skruczny?). Coat protein Sla1 thus
64 acts as a proxy for the behaviour of the plasma membrane. Membrane retraction, that is, inward
65 movement and subsequent retraction of the invaginated membrane back towards the cell wall is a
66 scission-specific phenotype (ref.Marko). Retraction rates do not increase in *vps1Δ* cells compared to
67 the WT (Fig.1C).

68
69
70 In order to study the total inward movement of the endocytic coat, and therefore the depth of
71 the endocytic invagination, the averaged centroid trajectory of 50 Sla1-eGFP patches (ref. Picco,
72 eLife 2015) in *vps1Δ* and WT cells is tracked and compared (Fig.1D). In brief: yeast cells expressing
73 fluorescently-tagged endocytic proteins are imaged at the equatorial plane. Since membrane
74 invagination progresses perpendicularly to the plane of the plasma membrane, proteins that move
75 into the cytoplasm during invagination do so in the imaging plane. Centroids of Sla1 patches- each
76 patch being an endocytic site- are tracked in time and averaged. This provides an average centroid
77 that can be followed with high spatial and temporal precision. For more details, refer to Picco et. al,
78 eLIFE 2015. Averaged centroid movement of Sla1-eGFP in WT cells is linear to about 140nm (Fig.1D).
79 Sla1 movement in *vps1Δ* cells has the same magnitude of movement (Fig.1D). In spite of slight
80 differences in the rates of movement, the total inward movement- and so the depth of endocytic
81 invagination- does not change.

82
83
84 Centroid tracking has shown that the number of molecules of Rvs167 peaks at the time of
85 scission, and is followed by a rapid loss of fluorescent intensity, simultaneous with a sharp jump
86 of the centroid into the cytoplasm (ref.Andrea). This jump, also seen in Rvs167-GFP kymographs
87 (Fig.1B), is interpreted as loss of protein on the membrane tube, causing an apparent spatial jump
88 to the protein localized at the base of the newly formed vesicle. Kymographs of Rvs167-GFP (Fig.1B),
89 as well as Rvs167 centroid tracking (Fig.1E) in Vps1 deleted cells show the same jump as in WT.

90
91
92 Since removal of the Rvs complex is known to increase the membrane retraction rate at endocytic
93 sites (ref Marko), involvement of the Rvs proteins in the scission process was investigated further.
94 The Rvs complex is composed of Rvs161 and Rvs167 dimers (ref.Dominik), so deletion of Rvs167
95 effectively removes both proteins from endocytic sites. We quantified the effect of *rvs167Δ* on
96 membrane invagination (Fig.1A-C). 27% of Sla1 patches move inward and then retract in *rvs167Δ*
97 cells (Fig.1C). Similar retraction rates were measured in other experiments (Kaksonen, Toret and
98 Drubin, 2005), and suggest failed scission in these 27% of endocytic events. Coat movement both of
99 retractions and of successful endocytic events were quantified (Fig.1F) as described in Picco et. al,
100 2015. Sla1 centroid movement in both successful and retracting endocytic events in *rvs167Δ* cells
101 look similar to WT up to about 50nm (Fig.1F). In WT cells, Abp1 intensity begins to drop at scission
102 time; similarly, in successful endocytic events, Abp1 intensity drops after Sla1 centroid has moved
103 about 100nm (Fig.1supplement), suggesting that scission occurs at invagination lengths between 60
104 -100 nm. That membrane scission occurs at shorter invagination lengths than in WT is corroborated
105 by the smaller vesicles formed in *rvs167Δ* cells by Correlative light and electron microscopy (CLEM)
106 (Kukulski et al., 2012). CLEM has moreover shown that Rvs167 localizes to endocytic sites after
107 the invaginations are about 60nm long (Kukulski et al., 2012). Sla1 movement in *rvs167Δ* indicates
108 therefore that membrane invagination is unaffected till Rvs is supposed to arrive. The Sla1 centroid

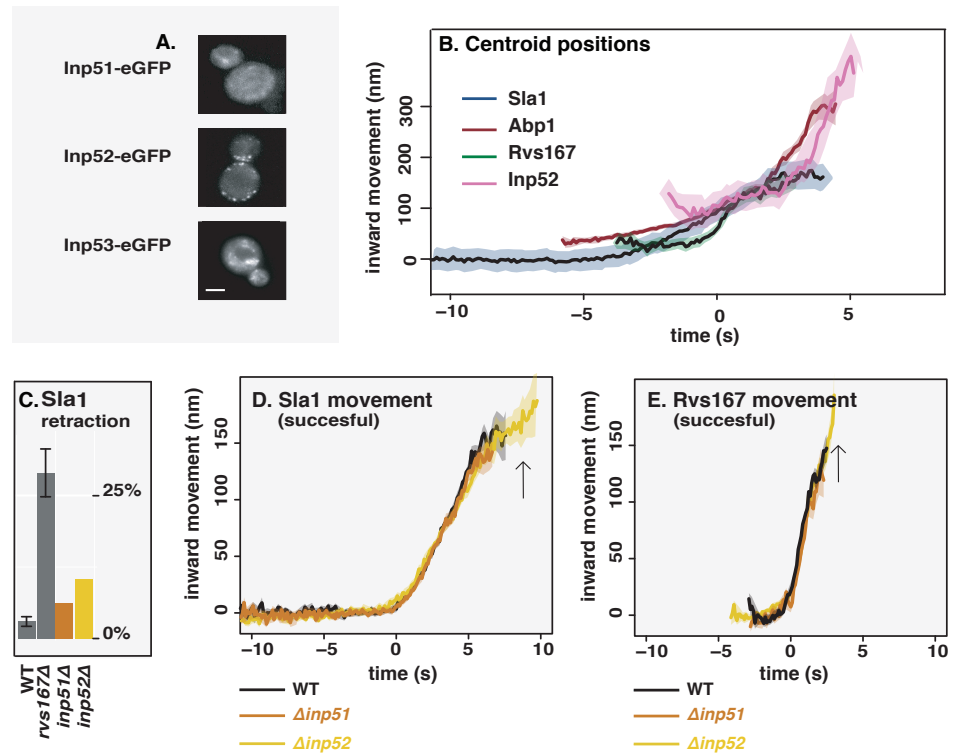


Figure 2. A. Cells with endogenously tagged Inp51, Inp52, and Inp53. B: Inp52 centroid trajectory is aligned in space and time to other endocytic proteins. C: Sla1 retraction rates in *inp51Δ* and *inp52Δ* cells compared to WT and *rvs167Δ*. Error bars are standard deviation from two data sets. D: Averaged centroid positions of Sla1-eGFP in WT, *inp51Δ*, and *inp52Δ* cells. E: Averaged centroid positions of Rvs167-eGFP in WT, *inp51Δ*, and *inp52Δ* cells.

for retraction events moves back towards its original position after inward movement.

Synaptojanins likely influence vesicle uncoating, but not scission dynamics.

Three Synaptojanin-like proteins have been identified in budding yeast: Inp51, Inp52, and Inp53. Inp51-eGFP exhibits a diffuse cytoplasmic signal, Inp52-eGFP localizes to cortical actin patches that are endocytic sites (Fig2 supplement) and Inp53 localizes to patches within the cytoplasm (ref). Spatial and temporal alignment of Inp52 with Sla1, Abp1, and Rvs167 (ref.Pico) shows that Inp52 protein molecules arrive in the late stage of endocytosis after Rvs167, and localizes to the invagination tip, suggesting a potential role in membrane scission (Fig.2b).

Inp53 was not investigated further, as its localisation conforms with other literature that find it is involved in the golgi trafficking pathway rather than endocytosis (ref Golgi). Although we were unable to see Inp51 localisation at endocytic sites, it may be recruited in small numbers below our detection limit. Deletion of Inp51 has been shown to exacerbate the effect of *inp52Δ* on membrane retraction (ref Liu), so both Inp51 and Inp52 were tested as potential candidates as scission regulators.

Dynamics of Sla1-eGFP and Rvs167-eGFP in either *inp51Δ* or *inp52Δ* cells were compared against the WT. Membrane retraction events do not significantly increase in either compared to the WT (Fig2c).

Magnitude and speed of Sla1 and Rvs167 centroid movement in *inp51Δ* is the same as the WT (Fig2.d, e). In *inp52Δ* cells, Sla1 movement also has the magnitude and speed as WT, but Sla1-eGFP signal is persistent after membrane scission (Fig.2d, arrow). Similarly, although Rvs167 inward movement looks similar to WT in *inp52Δ* (Fig2e), Rvs167-eGFP signal is persistent after inward

131 movement (Fig2e arrow), and Rvs167 and Sla1 disassembly has a delay (Fig2 supplement)

132 **Rvs BAR domains recognize membrane curvature in-vivo**

133 So far Rvs167 remains the protein that has a major influence on scission rates and inward moment
134 of Sla1. Recruitment of the Rvs complex to endocytic sites was thus investigated further. Interaction
135 between Rvs and membrane curvature in vivo has been indicated by work on other BAR domain
136 proteins (ref BAR), but has not so far been tested. In order to do so, we deleted the SH3 domain of
137 Rvs167 leaving the N-terminal BAR and GPA regions (henceforth BAR-GPA, Fig3a) and observed the
138 localization of the BAR region without SH3 influence. The GPA region is a disordered domain that
139 has no previously reported function (ref) and was retained to ensure proper folding and function
140 of the BAR domain. Endogenously tagged Rvs167-eGFP and BAR-GPA-eGFP colocalization with
141 Abp1-mCherry in WT and *sla2Δ* cells were compared (Fig3b). Sla2 acts as the molecular linker
142 between forces exerted by the actin network and the plasma membrane (ref. Skruzny). *sla2Δ* cells
143 therefore contain a polymerizing actin network at endocytic patches, but the membrane has no
144 curvature, and endocytosis fails. In these cells, the full-length Rvs167 protein co-localizes with
145 Abp1-mCherry, indicating that it is recruited to endocytic sites (Fig3b, "*sla2Δ*"). BAR-GPA localization
146 is removed, except for rare transient patches that do not co-localize with Abp1-mCherry.

147 **Rvs SH3 domains have an actin and curvature independent localisation**

148 The SH3 domain has known genetic interactions with actin-related endocytic proteins. In order to
149 test if these interactions are prevalent in vivo, we tested the localisation of full-length Rvs167 and
150 BAR-GPA in LatA treated cells (Fig3b, "LatA"). Plasma membrane localisation of full-length Rvs167
151 remains upon LatA treatment, and transient patches continue to exist in *sla2Δ* cells treated with
152 LatA (Fig3b, "*sla2Δ*+ LatA"). BAR-GPA localisation on the other hand, is removed in both.

153 **SH3 domains are likely recruited by Myosin 3**

154 Type I myosins Myo3 and Myo5, and Vrp1 have genetic or physical interactions with Rvs167 SH3
155 domains (Lila and Drubin, 1997; Colwill et al., 1999; Madania et al., 1999; Liu et al., 2009). We tested
156 the interaction between these proteins and the Rvs167 SH3 region by studying the localization
157 of full-length Rvs167 in cells with one of these proteins deleted, and treated with LatA. By LatA
158 treatment we expected to produce the situation in which BAR-curvature interaction is removed
159 (Fig3b). Then if we lost SH3 interaction because we deleted the protein with which it interacts, we
160 would lose localisation of Rvs167 completely. Deletion of neither Vrp1 nor Myo5 in combination
161 with LatA treatment removes the localization of Rvs167. Deletion of Myo3 with LatA treatment
162 removes localization of Rvs167.

163 **what about the differences in myo5 and myo3 number...**

164 **Loss of Rvs167 SH3 domain affects coat and actin dynamics**

165 Since the Rvs167 SH3 domain appears to have an important influence on the recruitment of the
166 Rvs complex to endocytic sites, we wondered if the domain had also an influence on endocytic
167 dynamics. We compared dynamics of Sla1 in WT and BAR-GPA strains, as well as Rvs167 and
168 BAR-GPA centroids (Fig4). Movement of Sla1 centroid is reduced in BAR-GPA cells (Fig4a). Tubular
169 invaginations are formed in BAR cells, and qualitatively resemble that in WT cells, as seen by CLEM
170 (Fig.4 supplement). Recruitment of BAR-GPA molecules is delayed compared to Rvs167. Rvs167
171 arrives to the invaginated tube about 30nm away from the Sla1 centroid position. The BAR-GPA
172 centroid is at the same 30nm away from the Sla1 centroid: it is likely that the delay in BAR-GPA
173 recruitment is delayed because the Sla1 movement is slowed down, and BAR-GPA molecules
174 recognize a specific geometry of invagination.

175 The inward jump of BAR-GPA is less than that of full-length Rvs167 (Fig.4b). Recruitment of BAR
176 is reduced to half that of Rvs167 (Fig4c), although cytoplasmic concentration of Rvs167 and BAR
177 are not different (Fig4 supplement). We also quantified the number of Abp1 and Rvs molecules

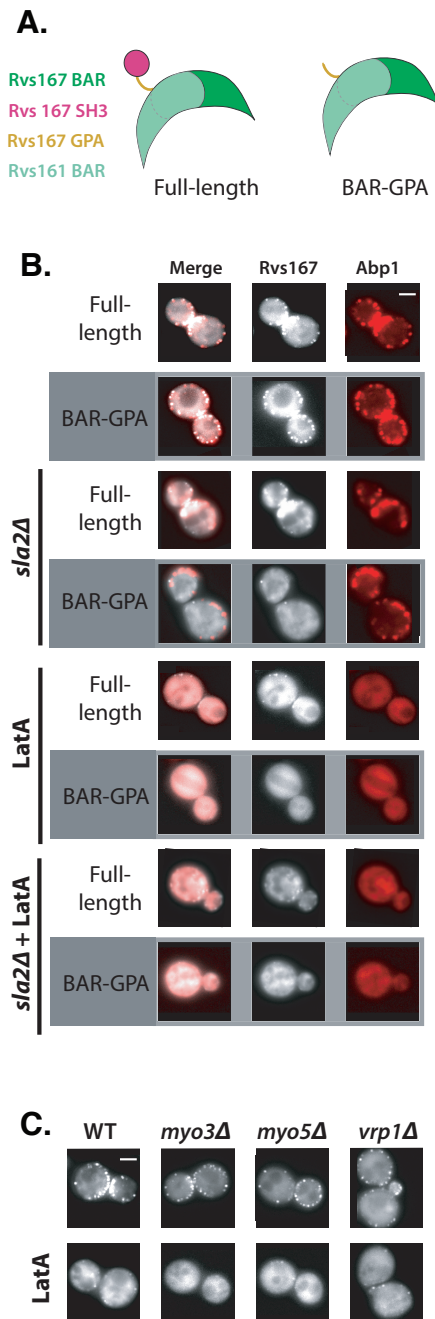


Figure 3. A: Schematic of Rvs protein complex with and without the SH3 domain. B: Localization of full-length and BAR-GPA in WT, *sla2Δ*, LatA treated, and LatA treated *sla2Δ* cells. C: Localization of full-length Rvs167-eGFP in WT, *myo3Δ*, *myo5Δ*, and *vrp1Δ* cells. Scale bars=2μm.

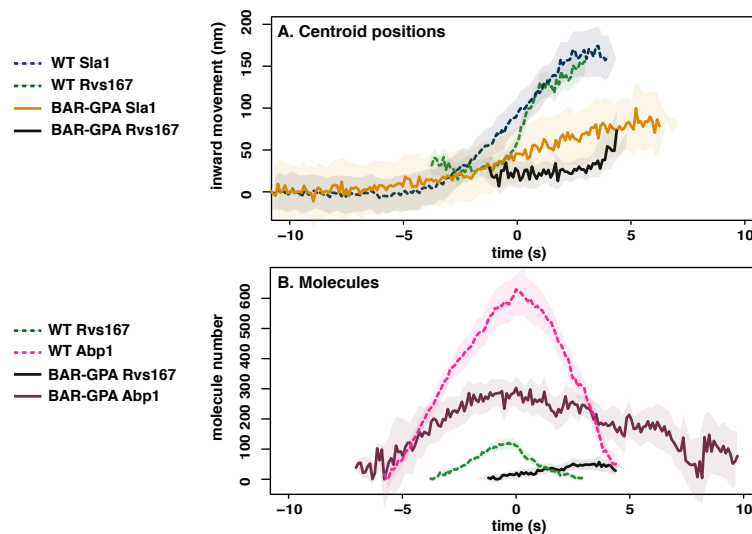


Figure 4. A: Averaged centroid positions aligned in space and time so that time=0(s) is the peak of fluorescent intensity of Abp1 in WT and BAR-GFP strains. B: Numbers of molecules of in WT and BAR-GPA strains, aligned so that time=0(s) is the peak of fluorescent intensity of Abp1 in the corresponding strains.

178 recruited to endocytic sites (Fig4b). Abp1 disassembly is slowed down in BAR-GPA cells compared to
 179 WT (Fig4b), and recruitment is reduced to 50% of WT recruitment (Fig.4c), likely indication disruption
 180 of actin network assembly.

181 **N-helix and GPA domains do not contribute to recruitment of Rvs or membrane** 182 **movement**

183 Etiam euismod. Fusce facilisis lacinia dui. Suspendisse potenti. In mi erat, cursus id, nonummy
 184 sed, ullamcorper eget, sapien. Praesent pretium, magna in eleifend egestas, pede pede pretium
 185 lorem, quis consectetur tortor sapien facilisis magna. Mauris quis magna varius nulla scelerisque
 186 imperdiet. Aliquam non quam. Aliquam porttitor quam a lacus. Praesent vel arcu ut tortor cursus
 187 volutpat. In vitae pede quis diam bibendum placerat. Fusce elementum convallis neque. Sed dolor
 188 orci, scelerisque ac, dapibus nec, ultricies ut, mi. Duis nec dui quis leo sagittis commodo.

189 **Reduced BAR domain recruitment corresponds to reduced membrane movement**

190 We wondered if the decreased Sla1 movement in BAR-GPA cells (Fig4a) was induced by loss of an
 191 SH3 domain mediated interaction, or because the BAR-GPA mutant is recruited in smaller numbers
 192 to endocytic sites. To check whether increasing the recruitment of the Rvs complex can rescue
 193 reduced Sla1 movement, Rvs167 and Rvs161 genes were duplicated endogenously (ref Huber) in
 194 diploid and haploid yeast cells. In haploid cells, increasing the number of Rvs167 and Rvs161 genes
 195 results in increased recruitment of Rvs167 to about 1.6 times the WT amount (Fig5c). Sla1 dynamics
 196 remains the same as in the WT (Fig5a). Duplicating the BAR-GPA domain alone increases the amount
 197 of BAR-GPA molecules recruited to endocytic sites (Fig5c), and rescues the loss of Sla1 movement in
 198 the 1x BAR-GPA, as well the inward jump of BAR-GPA itself (Fig5a,b). By gene duplication, diploid
 199 cells are generated containing either 4 copies of both Rvs genes, 2 copies of each gene (WT diploid),
 200 or 1 copy (by deleting one copy of Rvs167 and Rvs161). In diploid cells (Fig5d-f), amount of Rvs167
 201 recruited to sites increases with gene copy number (Fig5f). Adding excess Rvs to endocytic sites in
 202 the 4x case does not change the rate or total inward movement of Sla1, or of Rvs167 (Fig5d,e). In
 203 the case of 1x Rvs, Sla1 movement is slightly reduced after 100nm (Fig5a). Magnitude of Rvs167
 204 inward movement is unchanged, but the Rvs167-eGFP signal is lost immediately after the inward
 205 movement, unlike in the 4x and 2x cases. We measured the total number of Abp1 molecules at
 206 endocytic sites for different strains (Fig5g,h), and found that higher Abp1 numbers corresponds to

larger Sla1 centroid movement. Total Abp1 numbers recruited are reduced for 1xBAR and *rvs167Δ* strains (Fig5g,h), suggesting a correlation between the maximum number of Abp1 recruited and total invagination length

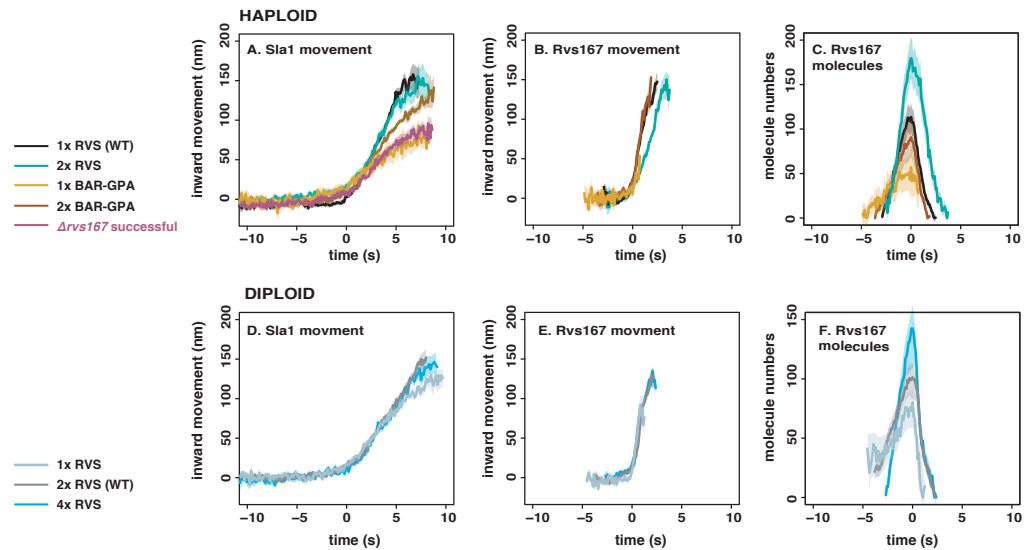


Figure 5. A half-columnwidth image using wrapfigure, to be used sparingly. Note that using a wrapfigure before a sectional heading, near other floats or page boundaries is not recommended, as it may cause interesting layout issues. Use the optional argument to wrapfigure to control how many lines of text should be set half-width alongside it.

Discussion

Recruitment and function of the Rvs complex in has been explored in this work, as well as several models for how membrane scission could be effected in yeast endocytosis. We propose that Rvs is recruited to endocytic sites by interactions between the Rvs BAR domains and invaginated membrane, and that SH3 domain mediated protein-protein interactions are required for efficient recruitment of Rvs to sites. Arrival of Rvs on membrane tube scaffolds the membrane and prevents premature membrane scission. Effective scaffolding depends on recruitment of a critical number of Rvs molecules. Rvs is a relatively short-lived protein at endocytic sites. It is recruited only once membrane tube is formed (Kaksonen, Toret and Drubin, 2005; Kukulski et al., 2012; Picco et al., 2015). FCS measurements (Boeke et al., 2014) have shown that the cytosolic concentrations of Rvs167 and Rvs161 are high (354nM and 721nM respectively) compared to other endocytic proteins like Las17, Vrp1, Myo3, and Myo5 (80-240nM). In spite of this, relatively few numbers of Rvs are recruited to endocytic sites, suggesting that recruitment is tightly regulated. In the case of Rvs, both timing and efficiency appear crucial to its function, the question is what confers both.

BAR domains sense *in vivo* membrane curvature and time recruitment of Rvs

The curved structure of BAR dimers (Peter et al., 2004; Mim et al., 2012) has suggested that Rvs is recruited by its preference for some membrane shapes over others, supported by its arrival at curved membrane tubes. In the absence of membrane curvature, in *sla2Δ* cells, the BAR domain alone does not localize to cortical patches (Fig.3b,c). This demonstrates for the first time that the BAR domain does indeed sense and requires membrane curvature to localize to cortical patches. Work on BAR domains have proposed that electrostatic interactions at the concave surface and tips of the BAR domain structure mediate membrane binding (Qualmann, Koch and Kessels, 2011).

232 Mutations in these lipid-binding surfaces would clarify the interaction with underlying lipids, and
 233 test if Rvs relies on similar interactions. BAR is able to localize to endocytic sites, and has a similar
 234 lifetime in WT cells (Fig4b). However, time alignment with Abp1 shows that there is a delay in the
 235 recruitment of BAR-GPA compared to Abp1 arrival, compared to full-length Rvd167 (Fig4c). The
 236 delayed recruitment occurs because the invagination takes longer to reach a particular length: Sla1
 237 moves inwards at a slower rate in BAR cells, and it takes longer for the membrane in BAR-GPA cells
 238 to reach the same length as Rvs167. Rvs167 arrives in BAR cells when Sla1 has moved inwards
 239 25-30nm (dashed red lines in Fig.4a), which is also the distance Sla1 has moved when Rvs167 arrives
 240 in WT. By the time Sla1 has moved this distance, the membrane is already tubular (Kukulski et
 241 al., 2012; Picco et al., 2015), consistent with Rvs arrival at invaginated tubes. This suggests Rvs
 242 recruitment is timed to specific membrane invagination length- therefore to a specific membrane
 243 curvature- and that this timing is provided by the BAR domain.

244 **SH3 domains allow efficient and actin independent recruitment**

245 Rvs167 in BAR cells accumulates to about half the WT number (Fig.3c), even though the same cyto-
 246 plasmic concentration is measured (supplement Fig3?), indicating that the SH3 domain increases
 247 the efficiency of recruitment of Rvs. In *sla2Δ* cells, full-length Rvs can assemble on the membrane
 248 (Fig.3b,c). Since BAR domains alone do not localize to patches in *sla2Δ* cells, full-length localiza-
 249 tion must be mediated by the SH3 domain, supporting a role for the SH3 domain in increasing
 250 recruitment of Rvs by clustering protein molecules. That full-length Rvs167 is able to assemble and
 251 disassemble at cortical patches in *sla2Δ* cells without the curvature- dependent interaction of the
 252 BAR domain (Fig.3b,c) indicates that the SH3 domain is able to mediate both the recruitment and
 253 the disassembly of Rvs at the endocytic site. In *sla2Δ* cells treated with LatA (Fig.3c), actin-based
 254 membrane curvature is inhibited, and the actin patch proteins are removed from the plasma mem-
 255 brane. Full-length Rvs167 in these cells still shows transient localizations at the plasma membrane.
 256 In *sla2Δ* cells treated with LatA, the localization of BAR is lost. This suggests that localization of the
 257 full-length Rvs167 in LatA treated cells is dependent on an SH3 domain interaction, and that this is
 258 independent of both actin and membrane curvature.

259 In WT cells, the Abp1 and Rvs167 fluorescent intensities reach maxima concomitantly (Fig4b),
 260 and the consequent decay of both also coincide. Coincident disassembly indicates that upon vesicle
 261 scission, the actin network is immediately disassembled. Membrane scission essentially occurs
 262 around the intensity peak of the two proteins. This coincident peak is lost in BAR-GPA cells: BAR-
 263 GPA-eGFP in these cells peaks several seconds after Abp1 intensity starts to drop, and the decay of
 264 Abp1 is prolonged, taking nearly double the time as in WT. The number of Abp1 molecules recruited
 265 is decreased to about two thirds the WT number. Although it is not clear what the decoupling of
 266 Abp1 and Rvs peaks means, the changes in Abp1 dynamics suggests a strong disruption of the actin
 267 network dynamics. SH3 domains are known to interact with components of the actin network like
 268 Abp1 and Las17 (Lila and Drubin, 1997, Madania et al., 1999), but study of other components of
 269 the actin machinery will be required to understand how exactly loss of the SH3 has changed the
 270 progression of endocytosis.

271 SH3 interaction with an endocytic binding partner likely help recruit Rvs to endocytic sites. Many
 272 such interaction partners have been proposed. Abp1 interaction with the Rvs167 SH3 domain
 273 has been shown (Lila and Drubin, 1997; Colwill et al., 1999), as has one with WASP protein Las17
 274 (Madania et al., 1999; Liu et al., 2009), yeast Calmodulin Cmd1 (Myers et al., 2016), type I myosins
 275 (Geli et al., 2000), and Vrp1 (Lila and Drubin, 1997). All of these suggested binding partners localize
 276 to the base of the invagination (Yidi Sun, 2006; Picco et al., 2015), and do not follow the invaginating
 277 membrane into the cytoplasm. The SH3 interaction partner is likely Myo3 (Fig3d), and SH3 domains
 278 interact with the endocytic network at the base of the invagination. Centroid tracking however,
 279 suggests that Rvs is accumulated all over the membrane tube. If Rvs was recruited to the base and
 280 pulled up as the invagination grows, the centroid would move continuously upwards rather than
 281 remain relatively non-motile before the jump at scission time. It is possible that the SH3 initially

282 helps cluster near the base, and as the membrane invaginations grow longer, BAR-membrane
283 interactions dominate.

284 **Accumulation of Rvs on membrane invagination**

285 When ploidy is doubled from haploid to diploid yeast cells, we could expect that double the protein
286 amount is expressed and recruited, but it does not appear so. The amount of Rvs recruited in
287 WT haploid and diploids remains about the same, and cytoplasmic signal is similar (Fig.5, Fig5
288 supplement). This invariance between accumulated protein in haploids and diploids shows that Rvs
289 recruitment is not determined by the number of alleles of Rvs. Haploid and diploid cells appear
290 to tune the amount of Rvs recruitment to get a specific amount to endocytic sites. WT diploids
291 (2xd) contain two copies each of RVS161 and RVS167 genes. Rvs duplicated diploids, which contain
292 four copies each of RVS167 and RVS161 (4xd) could be expected to express and recruit to sites
293 twice the amount of Rvs as 2xd. However, compared to 2xd, cytoplasmic signal in 4xd increases
294 by 1.6x and recruitment of Rvs167 to endocytic sites increases only by 1.4x. Doubling the gene
295 copy number increases, but does not double protein expression or recruitment in the case of
296 Rvs. Similarly, duplicating Rvs genes in haploid cells results in an increase in number of molecules
297 recruited, but not in doubling (1xh, 2xh). Although the rate of adding Rvs is different in haploids and
298 diploids, in both cases, it increases by gene copy number (yellow line in Fig.4.2). Cytoplasmic protein
299 concentration is increased when gene copy number is increased, and recruitment to endocytic
300 sites is increased by the increase in cytoplasmic concentration. These data suggest that the amount
301 of Rvs that is recruited scales with available concentration of protein. Comparing across ploidy
302 however, the rate of Rvs recruitment is lower in WT diploid compared to WT haploid (2xd vs 1xh,
303 Fig.4.1)

304 for this is not clear. 4.2 Arrangement of Rvs dimers on the membrane A homology model of
305 the Rvs BAR dimer structure based on Am- phiphysin suggests that it has the concave structure
306 typical for N- BAR domains. Rvs is a hetero- rather than homodimer unlike Am- phiphysin, and a
307 high-resolution structure will be necessary to clarify the interaction and arrangement of Rvs on
308 endocytic tubes. There are some indications from the experiments in this thesis however, regarding
309 its interaction with the membrane. 4.2.1 Rvs does not form a tight scaffold on membrane tubes
310 Observations of in vitro helices of BAR domains have suggested that Rvs might form a similar helical
311 scaffold. The number of Rvs molecules recruited to endocytic sites is high enough to cover the
312 surface area of the tubular invagination, so it has been proposed that an Rvs scaffold covers the
313 entire membrane tube up to the base of the future vesicle (Picco et al., 2015). In Rvs duplicated
314 diploid cells (4xd), Rvs can be recruited at a much faster rate than in the WT (2xd) (Fig.3.10B-
315 C, Fig.4.2) while disassembly dynamics is the same in both (Fig.3.10C, Fig.4.3). The exponential
316 decay of fluorescent intensity in WT haploid and diploid cells (1xh, 2xd, Fig.4.3) indicates that
317 all of the protein is suddenly disassembled from the endocytic site. When the membrane tube
318 undergoes scission, there is no more tubular curvature for the Rvs to bind to. The sharp decay is
319 therefore consistent with a BAR scaffold that breaks upon vesicle scission because there is no more
320 membrane interaction, releasing all the membrane-bound protein at once. A similar decay in the
321 4xd strain suggests that all the Rvs in this case is also bound to the membrane: if the protein was
322 not bound to the membrane, fluorescent intensity would not decay sharply. Since the membrane is
323 able to accommodate 1.4x the amount of BAR protein as the WT, it would suggest that at lower
324 protein amounts, a tight helix that covers the entire tube is not likely. Adding molecules to a tube
325 already completely covered by a scaffold would result in a change in Rvs assembly and disassembly
326 dynamics. Further, additional molecules would have to be added at the top or base of a tight
327 scaffold. At the top, the radius of curvature is decreased compared to the tube since this is the
328 rounded vesicle region. At the base, the plasma membrane is nearly flat, and the Rvs BAR domain
329 is similarly unlikely to favour interactions here. Otherwise the scaffold would have to be disrupted
330 to add new molecules, which would likely slow down recruitment rate rather than speed it up.
331 Molecules could also be added concentric to an existing scaffold. However, the concave surface of

Rvs is known to interact with lipids, and multiple layers of BAR domains on the membrane tube would probably not show the sudden disassembly seen here. I assume that the membrane surface area does not change in the 4xd compared to 2xd from the identical movement of Sla1 in both cases (Fig.3.10A). It is possible that a wider tube is formed, which would increase the membrane surface area for BAR binding. This would, however, require the BAR domains to interact with a lower radius of curvature than in WT. This seems unlikely, and in the absence of any indication otherwise, I assume that the membrane tubes in all diploid and haploid cases have the same width. 4.2.2 A limit for how much Rvs can be recruited to the membrane In the case of Rvs duplication in haploids (2xh), a change in disassembly dynamics is seen (Fig.3.9C, Fig.4.3). In 2xh, the maximum number of molecules recruited is 178 ± 7.5 compared to the maximum of 113.505 ± 5.2 in WT (1xh). This means that nearly 1.6x the WT amount of protein is recruited to membrane tubes in the 2xh case. The Rvs167 fluorescent intensity in 2xh shows a delay in disassembly. This suggests that the excess protein may not be directly on the membrane, since if the protein was membrane bound, when the membrane breaks, the protein must be released. The excess Rvs could either interact with the actin network via the SH3 domain, or interact with other Rvs dimers. By a similar argument as in 4.2.1 above, I do not expect that multiple layers of BAR domains are formed, and that the excess protein is recruited by the interaction of the SH3 domain. Another explanation for the delayed disassembly is that at high concentrations of Rvs like in the 2xh case, a tight BAR scaffold is formed, and the BAR domains interact with adjacent BAR domains. When the membrane undergoes scission, the protein is no longer membrane-bound, but lateral interactions delay disassembly of the scaffold. Lateral interactions between neighbouring BAR dimers have been shown in the case of Endophilin (Mim et al., 2012). It is not currently clear where the Rvs molecules are added in the 2xh case: superresolution microscopy could clarify whether it is added at the membrane tube. Whatever the arrangement of the Rvs complex on the membrane, disassembly dynamics is changed in the case of 2xh, compared to the other haploid and diploid strains. Since the number of Rvs molecules is highest in this strain, this suggests that there is a limit to how much Rvs can assemble on the tube without altering interaction with the endocytic protein network. 4.2.3 Conclusions for Rvs localization All of these data support the idea that Rvs recruitment rate and total numbers are determined by concentration of protein in the cell. The maximum number of molecules that can interact with the membrane is limited by the surface area of the invagination. Although more can be recruited, Rvs molecules over a certain threshold interact in a different way with endocytic sites, possibly via the SH3 domain. Timing of recruitment to sites is by curvature-recognition via the BAR domain, while efficiency of recruitment and interaction with the actin network is established via the SH3 domain. 4.3 What causes membrane scission?

Rvs acts as a membrane scaffold preventing membrane scission

Invaginations in *rvs167Δ* cells undergo scission at short invagination lengths of about 80nm (Fig.3.2), compared to the WT lengths of 140nm. This shows that first, enough forces are generated at 80nm to cause scission. Then, that Rvs167 is required at membrane tubes to prevent premature scission. Prevention of scission at short invagination lengths can be explained by Rvs stabilizing the membrane invagination via membrane interactions of the BAR domain (Boucrot et al., 2012; Dmitrieff and Nedelec, 2015). Rvs preventing membrane scission could also be explained by the SH3 domain mediating actin forces to the invagination neck: one can imagine that the SH3 domain somehow decouples actin forces from the neck, and that this delays scission. Since invagination lengths of *rvs167a* cells are increased towards WT by overexpression of the BAR domain alone (Fig.3.12A), I propose that localization of Rvs BAR domains to the membrane tube stabilizes the membrane. This allows deep invaginations to grow until actin polymerization produces enough forces to overcome this stabilization and sever the membrane. Stabilization of the membrane tube increases with increasing amounts of BAR domains recruited to the membrane tube (Fig.3.12). The requirement for Rvs scaffolding cannot be removed by reducing turgor pressure (Fig.3.13), suggesting that the function of the scaffold is not to counter turgor pressure.

382

383 Scission efficiency decreases with decreased amounts of Rvs: in diploids, lowering the amount
 384 of Rvs by 20 molecules decreases scission efficiency to about 90% from 97%. This indicates that
 385 a particular coverage of the membrane tube is required for effective scaffolding by BAR domains.
 386 In support of this, in BAR strains, fewer numbers of Rvs are recruited, and scission efficiency is
 387 similarly reduced. At low concentrations of Rvs like in the 1xd cells, it is likely that some membrane
 388 tubes recruit the critical number of Rvs, in which case the invaginations grow to near WT lengths.
 389 Over a certain amount of Rvs, adding more BAR domains does not increase the stability of the
 390 tube: in 4xd, the same amount of actin is recruited before scission as in the 2xd and 1xd strains. If
 391 enough forces are generated at 80nm, why is scission efficiency decreased in *rvs167Δ* compared
 392 to WT? Forces from actin may be at a threshold when the invagination is at 80nm. There could be
 393 enough force to sever the membrane, but not enough to sever reliably. The Rvs scaffold then keeps
 394 the network growing to accumulate enough actin to reliably cause scission. Controlling membrane
 395 tube length could also be a way for the cell to control the size of the vesicles formed, and therefore
 396 the amount of cargo packed into the vesicle.

397 **What causes membrane scission?**

398 We have tested several scission models that include a major role for the Rvs complex. The seemingly
 399 obvious solution to the scission problem is the action of a dynamin-like GTPase. If loss of the yeast
 400 Dynamin Vps1 prevented or delayed scission, the membrane would continue to invaginate longer
 401 than WT lengths, and Sla1 movements of over 140nm should be observed. Rvs centroid movement
 402 would likely also be affected: a bigger jump inwards could indicate that a longer membrane has
 403 been cut. That neither is seen in the behaviour of coat and scission markers indicates that even if
 404 Vps1 is recruited to endocytic sites, it is not necessary for Rvs localization or function, and is not
 405 necessary for scission. The Inp51, Inp52 data tests the lipid hydrolysis model, in which synaptojanins
 406 hydrolyze PIP2 molecules that are not covered by BAR domains, resulting in a boundary between
 407 hydrolyzed and non- hydrolyzed PIP2. This model predicts that interfacial forces generated at the
 408 lipid boundary causes scission (Liu et al., 2006). Inp51 is not seen in patches at the cellular cortex,
 409 but this could be because protein recruitment is below our detection threshold. Inp52 localizes to
 410 the top of invaginations right before scission, consistent with a role in vesicle formation (Fig.3.7D).
 411 Some predictions of the lipid hydrolysis model are inconsistent with our data, however. First, vesicle
 412 scission is expected to occur at the interphase of the hydrolyzed and non-hydrolyzed lipid. Since the
 413 BAR scaffold covers the membrane tube, this interphase would be at the top of the area covered by
 414 Rvs. Kukulski et al., 2012 have shown that vesicles undergo scission at 1/3 the invagination length
 415 from the base: that is, vesicles generated by the lipid boundary would be smaller than have been
 416 measured. Second, removing forces generated by lipid hydrolysis by deleting synaptojanins should
 417 increase invagination lengths, since scission would be delayed or it would fail without those forces.
 418 Deletion of neither Inp51 nor Inp52 changes the invagination lengths: Sla1 movement does not
 419 increase. That the position of the vesicle formed is also unchanged compared to WT is indicated by
 420 the similar magnitude of the jump into the cytoplasm of the Rvs centroid. There are some changes
 421 in the synaptojanin deletion strains (Fig.3.8). In *inp51Δ* cells, Rvs assembly is slightly slower than
 422 that in WT. Therefore, Inp51 could play a role in Rvs recruitment. In the *inp52Δ* strain, about 12% of
 423 Sla1-GFP tracks retract, indicated that scission fails in those cases. Although this is low compared to
 424 the failed scission rate of *rvs167Δ* cells (close to 30%), this data could suggest a moderate influence
 425 of Inp52 on scission. Rvs centroid persists after scission for about a second longer in *inp52Δ* cells
 426 than in WT, indicating that disassembly of Rvs on the base of the newly formed vesicle is delayed.
 427 Inp52 is likely involved in vesicle un- coating Deletion of synaptojanin-like Inp52 does not affect the
 428 movement of the invagination. In spite of this, Sla1 patches persist for longer after scission in the
 429 *inp52Δ* than in WT cells, as does Rvs167, indicated by the arrows in Fig.3.8A,D. Persistence of both
 430 suggests that rather than the scission timepoint, post-scission disassembly of proteins from the
 431 vesicle is inhibited in *inp52Δ* cells. Inp52 then plays a role in recycling endocytic proteins from the

vesicle to the plasma membrane. The slower assembly of Rvs in *inp51Δ* and the increase in coat retraction rates of *inp52Δ* could indicate that there is a slight effect on Rvs recruitment, and that lipid hydrolysis could play a small role in scission.

Protein-friction mediated membrane scission proposes that BAR domains induce a frictional force on the membrane, causing scission. In Rvs duplicated haploid cells (2xh), adding up to 1.6x the WT (1xh) amount of Rvs to membrane tubes does not affect the length at which the membrane undergoes scission (Fig.3.9). If more BAR domains were added to the membrane tube, frictional force generated as the membrane is pulled under it should increase, and the membrane should rupture faster. That is, membrane scission occurs as soon as WT forces are generated on the tube. Since BAR domains are added at a faster rate in the 2xh cells, these forces would be reached at shorter invagination lengths. In 2xh cells, WT amount of Rvs is recruited at about 1.8 seconds before maximum fluorescent intensity, but scission does not occur at this time. Instead, Rvs continues to accumulate, and the invagination continues to grow. In diploid strains, adding 1.4x the WT amount of Rvs in the 4x Rvs case also does not change length of membrane that undergoes scission. Therefore, protein friction due to Rvs does not appear to contribute significantly to membrane scission in yeast endocytosis.

Maximum amount of Abp1 measured in all the diploid strains is about 220 molecules (Fig.3.11). In this case, only one allele of Abp1 is fluorescently tagged, so half the amount of Abp1 recruited is measured. The maximum amount of Abp1 recruited is then double that measured, which is about 440 ± 20 molecules (assuming equal expression and recruitment of tagged and untagged Abp1). In WT haploid cells, the maximum number of Abp1 measured is 460 ± 20 molecules. That the same number of molecules of Abp1 is recruited in all cases before scission indicates that scission timing depends on the amount of Abp1, and hence, on the amount of actin recruited. This data is consistent with actin supplying the forces necessary for membrane scission. The membrane invagination continues until the “right” amount of actin is recruited. At this amount of actin, enough forces are generated to rupture the membrane. The amount of force necessary is determined by the physical properties of the membrane like membrane rigidity, tension, and proteins accumulated on the membrane (Dmitrieff and Needeelec, 2015). Vesicle scission releases membrane-bound Rvs, resulting in release of the SH3 along with BAR domains. Release of the SH3 domains could indicate to its binding partner in the actin network that vesicle scission has occurred, beginning disassembly of actin components. In BAR strains, a low amount of actin is recruited (Fig.3.4C). Although the absence of the SH3 domain severely perturbs the actin network, the mechanistic effect of this perturbation is unclear.

Model for membrane scission

I propose that Rvs is recruited to sites by two distinct mechanisms. SH3 domains cluster Rvs at endocytic sites. This SH3 interaction increases the efficiency with which the BAR domains sense curvature on tubular membranes. BAR domains bind to endocytic sites by sensing tubular membrane. BAR domains are recruited over the entire membrane tube, but do not form a tight helical scaffold. Membrane shape is stabilized against fluctuations that could cause scission by the BAR-membrane interaction. This prevent actin forces from rupturing the membrane, and the invaginations continue to grow in length as actin continues to polymerize. BAR recruitment to membrane tubes is restricted by the surface area of the tube: after a certain amount of Rvs, the excess interacts with endocytic sites via the SH3 domain. Adding over a certain amount of Rvs also does not increase the stabilization effect on the tube. As actin continues to polymerize, at a certain amount of actin, enough forces are generated to overcome the resistance to membrane scission provided by the BAR scaffold. The membrane ruptures, and vesicles are formed. Synaptojanins may help recruit Rvs at endocytic sites: Inp51 and Inp52 have proline rich regions that could act as binding sites for Rvs167 SH3 domains. They are involved in vesicle uncoating post-scission, likely by dephosphorylating PIP2 and inducing disassembly of PIP2-binding endocytic proteins. Eventually

482 phosphorylation regulation allows endocytic proteins to be reused at endocytic sites, while the
483 vesicle is transported elsewhere into the cell.

484 Morbi luctus, wisi viverra faucibus pretium, nibh est placerat odio, nec commodo wisi enim eget
485 quam. Quisque libero justo, consectetur a, feugiat vitae, porttitor eu, libero. Suspendisse sed
486 mauris vitae elit sollicitudin malesuada. Maecenas ultricies eros sit amet ante. Ut venenatis velit.
487 Maecenas sed mi eget dui varius euismod. Phasellus aliquet volutpat odio. Vestibulum ante ipsum
488 primis in faucibus orci luctus et ultrices posuere cubilia Curae; Pellentesque sit amet pede ac sem
489 eleifend consectetur. Nullam elementum, urna vel imperdiet sodales, elit ipsum pharetra ligula,
490 ac pretium ante justo a nulla. Curabitur tristique arcu eu metus. Vestibulum lectus. Proin mauris.
491 Proin eu nunc eu urna hendrerit faucibus. Aliquam auctor, pede consequat laoreet varius, eros
492 tellus scelerisque quam, pellentesque hendrerit ipsum dolor sed augue. Nulla nec lacus.

493 Methods and Materials

494 Guidelines can be included for standard research article sections, such as this one.

495 Nulla malesuada porttitor diam. Donec felis erat, congue non, volutpat at, tincidunt tristique,
496 libero. Vivamus viverra fermentum felis. Donec nonummy pellentesque ante. Phasellus adipiscing
497 semper elit. Proin fermentum massa ac quam. Sed diam turpis, molestie vitae, placerat a, molestie
498 nec, leo. Maecenas lacinia. Nam ipsum ligula, eleifend at, accumsan nec, suscipit a, ipsum.
499 Morbi blandit ligula feugiat magna. Nunc eleifend consequat lorem. Sed lacinia nulla vitae enim.
500 Pellentesque tincidunt purus vel magna. Integer non enim. Praesent euismod nunc eu purus.
501 Donec bibendum quam in tellus. Nullam cursus pulvinar lectus. Donec et mi. Nam vulputate metus
502 eu enim. Vestibulum pellentesque felis eu massa.

503 Citations

504 LaTeX formats citations and references automatically using the bibliography records in your .bib
505 file, which you can edit via the project menu. Use the `\cite` command for an inline citation, like
506 `?`, and the `\citep` command for a citation in parentheses (`?`). The LaTeX template uses a slightly-
507 modified Vancouver bibliography style. If your manuscript is accepted, the eLife production team
508 will re-format the references into the final published form. *It is not necessary to attempt to format*
509 *the reference list yourself to mirror the final published form.* Please also remember to **delete the line**
510 `\nocite{*}` in the template just before `\bibliography{...}`; otherwise *all* entries from your .bib
511 file will be listed!

512 Acknowledgments

513 Additional information can be given in the template, such as to not include funder information in
514 the acknowledgments section.